AIAA 96-3203

Evaluation of Diamond Grids for Ion Thruster Optics: Low Energy Sputter Yield Measurements

J.J. Blandino and D.G. Goodwin
Division of Engineering and Applied Science
California Institute of Technology
Pasadena, CA 91125

C.E. Garner
Jet Propulsion Laboratory
Pasadena CA 91109-8099

32nd AIAA/ASME/SAE/ASEE
Joint Propulsion Conference and Exhibit
July 1-3, 1996 / Lake Buena Vista, FL

AIAA 96-3203

Evaluation of Diamond Grids for Ion Thruster Optics: low Energy Sputter Yield Measurements

J. J. Blandino† and D. G. Goodwin‡
Division of Engineering and Applied Science
California Institute of Technology
Pasadena California 91125

C. E. Garner††
Jet Propulsion Laboratory
California Institute of '1'ethnology
Pasadena California91109

Abstract

Sputter yields have been measured for chemically-vapor deposited polycrystalline diamond, carbon-carlron composite, and molybdenum subject to bombardment with xenon ions at 150, ?50, 500, and 750 electron volts. The yields for molybdenum and carbon-carbon increased monotonically with energy, as expected, with values ranging from 0.36 at 150 eV to 1.4 al "150 eV for the molybdenum and ().1 3 to 0.2.6 for the carbon-carbon. The yield for the polycrystalline diamond was non-monotonic in energy, due most likely 10 the surface topography. The diamond yield ranged from ().1? to 0.33 over the range of energies investigated.

I. Introduction

In recent years there has been significant progress made in the production of chemically vapor deposited (CVD) diamond films. Improvements in quality, reproducibility, and growth rates (> 10 mm hr^{-1}) have made diamond films attractive for a variety of applications in the fields of electronics, optics, and tribology, among others [1]. One potential application under evaluation at the Jet Propulsion laboratory involves the use. of diamond films as coatings for ion accelerator electrodes which are subject to sputter erosion [2]. While much has been published in the CVD diamond literature regarding its electronic, optical, and mechanical properties, there. is relatively little in the way of sputter yields, and none to our knowledge specifically for bombardment with xenon at energies less than 1 keV.

The feasibility of using diamond films as an electrode material for ion thrusters is dependent upon a number of material properties in addition to the sputter yield. These include thermal conductivity, electrical conductivity, and coefficient of thermal expansion. These properties have been discussed in a previous paper [2] in addition to fabrication issue.s and relative erosion rates at energies of 500" and 750 cV. In this paper, wc present results for the at osolute sputter yield, and corresponding erosion rate, of diamond subject to xenon ion bombardment at energies of 150, 2S(), 500, and 750 eV. While. polycrystalline diamond was our primary interest, we were also interested in its yield relative to molybdenum and carbon-carbon composite, both in use as electrode materials.

II. Experiment

An important consideration when conducting sputter yield measurements is 10 minimize the influence of residual facility gases. Previous work suggests that the presence of nitrogen can lower the erosion rate of metals whereas oxygen has been shown to increase the erosion rates of carbon based materials. Reactive ion etching is onc technique which has been used successfully to etch structures in diamond. In this technique a NO_2 gas jet incident on a diamond surface is used while the target is under bombardment with ? keV xenon ions [4]. The incident ions in this case provide. the activation energy required to form ('() and CO_2 volatiles. Minimizing contamination is therefore essential to reduce the chances of reactively eroding the carbon targets and obtaining artificially high sputter yields. For these reasons the present test was conducted in a facility capable of relatively low ultimate. pressures.

The system used was an ultra-high-vacuum chamber with a 3 cm Kaufman ion soorcc (Commonwealth Scientific Corp.) normally used for sputter deposition. The vacuum chamber geometry is depicted in Fig. 2. The systc.in is pumped with a turbomolecular pump (1 15 L/sec) backed by a small mechanical pump (().8 L/sec) down into the 10^{-4} Pa (10^{-6} Torr) range and then with a 6" cryopump (1 S()() 1./see) to the 1()-7 Pa (1()-9 Torr) range. '1 The base and test pressures for each of the cam arc

† Graduate Student, Member AIAA.
‡ Associate Professor
†† Member of the Technical Staff, Advanced Propulsion Technology Group, Member AIAA.

summarized in '1 able 1. As an additional measure, the chamber was baked al over 1O() C every evening for several hours.

One drawback of using a chamber measuring approximately 12 inches high by 15 inches wide is the. relative in flexibility of sample and probe place.rncm. The sample.s were. located approximately ?.6 inches downstream of the source exit plane, Although this resulted in relatively high incident current densities, and hence shorter test ti mcs, it also resulted in some non-uniformity of the ion current profile over the samples.

The present experimental approach included centering the probe on the point of maximum current density in the beam. This also introduces a non-normal incidence angle into the experiment. In addition, divergence of the ion beam also increases the angle of incidence. The angle of the target mount with respect to the source center-line is listed in Table 1 along with the divergence angle. A reasonable estimate of the. incidence angle at the large.1 (measured from the surface normal) is the sum of time two angle.s. Unfortunately, wc do not have data for the mount angle cor lc'spending to the 500 CV case, but from the data at the other energies it is likely the mount angle was between 6 and 12 degrees. The incidence angle was therefore sonic.whc.rc in the range of 9 to 2.2 degrees allowing for the uncertainty in the dive.rgcncc angle..

III. Data Analysis

The present work utilized the technique where the. depth of the eroded valley in the target material is measured with a micro-stylus or profilometer. One assumption inherent in this approach is that the. valley depth represents an averaged volume removed per unit area where in fact it only represents the eroded profile. at the location where [he. trace is taken. A true average would require multiple profilometer scans and [hen an integration of the "slices" to calculate the eroded volume. The diagram in Fig. 1 illustrates the relevant dimensions used in the calculation of eroded depth. Measuring the depth only at the center of the valley does not adequately take into account the profile of the valley walls which may not be vertical. It was found that the molybdenum tended 10 have more vertical walls than the polycrystalline diamond in which the valley walls sloped gently. In order to calculate a sputtered volume per unit area, or mean effective depth, the depth profile was integrated according to

$$h_{eff} = \frac{1}{(x_r - x_l)} \int_{x_l}^{x_r} (y(x)_{mean} - y(x)_{valley}) dx \qquad (1)$$

The traces obtained from the profilometer were scanned into a computer and digitized. In addition to facilitating the integration in Eq. 1, this digitized mesa-valley-mesa profile could be subjected to statistical analysis 10 quantify surface roughness.

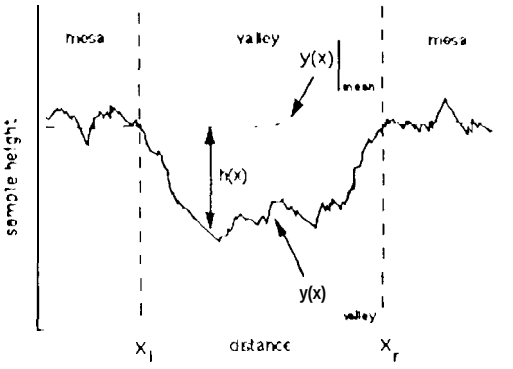

Fig. 1. Schematic of profilometer trace illustrating mesa curve fit which defines datum for depth measurements.

A least squares line fit through the mesa points establishes a datum, $y(x)_{mean}$, from which the valley depth at each x location can be measured. '1'here is a standard deviation associated with this iinc fit as a result of the mesa surface. roughness which is incorporated into the overall uncertainty estimate. The effective depth h_{eff} is then used 10 calculate the number N_A of target atoms removed per unit area;

$$N_A = \rho h_{eff} \frac{N_{avo}}{M} \qquad (2)$$

where N_{avo} is Avogadro's number, M the molecular weight, and ρ the target density. The values for the sample density used in calculating the yields were 10.2 g/cm^3 for molybdenum, 1.65 g/cm^3 for carbon-carbon, and 3.5 g/cm^3 for the CVD diamond Because of difficultly measuring the CVD sample volume the density was estimated to be that of single crystal diamond. SEM imaging of [he. sample did not reveal any evidence of porosity indicating this is a good assumption.

A planar probe was usc(1 to measure current incident on the target. This probe sur face was a 0.063" diameter tungsten disk which was biased to ?5 V Mow facility ground to repel electrons. There are several effects which contribute to the experimental uncertainty in the reported measurements. These include secondary electron emission from the probe as well as collection of doubly ionized gas atoms and charge exchange ions, The measured current was corrected for secondary electron emission using data from Ref. 3. This correction is small (1 .4-1.5 percent) for the tungsten probe used. A gas utilization efficiency and ratio of double 10 single ion current was calculated for each case using the methodology described in Ref. 10. The results of these calculations arc shown in Table 1.

Because the base pressure for these tests was relatively low, the dominant source of gas atoms which are available to become charge exchange ions will be the unionized xenon from the discharge chamber, a fraction of wb ich will drift out through the grids and into [be. beam. The ratio of the beam current 10 the total gas mas flow rate (expressed as a current) is the gas utilization efficiency. For commercial ion sources used primarily for sputter deposition (as opposed to propulsion), this efficiency can be quilt low mulling in significant loss of unionized gas through the grids. If the charge exchange current is a significant fraction of the collected current, a correction must be made to avoid overestimating the dosage of energetic sputtering ions. The total current collected at the probe is given by

$$J_p = J_b(1 + \gamma_2) + J_{cex}$$

where J_b is the energetic beam current, γ_2 the secondary electron emission coefficient, and J_{cex} the current due to charge exchange ions. Because one is really interested in dosages, the currents arc integrated over the duration of the exposure τ to obtain an expression for the total delivered charge Q_b due to beam ions.

$$Q_b = \frac{1}{1 + \gamma_2}\left[\int_0^\tau J_p(t)dt - \int_0^\tau J_{cex}(t)dt\right] \qquad (3)$$

The first integral in the brat.kc.(s represents the uncorrected, recorded probe. cur-rent. 'I'his was intc.grated graphically from the strip chart data for the probe. The second integral represents the dosage of charge exchange ions and generally is not known as a function of time.. Analysis willl~~:ir(iclc-ir]-cell (PIC) computer simulations were used to estimate the charge exchange current at least to the right order of magnitude. Based on these calculations a constant value for the charge exchange current equal to IO percent of the mean (averaged over the test duration) energetic current density was used.

Rc.cause the probe will count the arrival of a double ion as lwo single ions, it is necessary to calculate the equivalent single ion dosage at the target. In terms of the double 10 single ion current ratio

$$R_d = \frac{J_b^{++}}{J_b^{+}}$$

wc can express the dosage of single and double ions as

$$Q_b^{+} = \frac{1}{1 + R_d}Q_b \qquad Q_b^{++} = \frac{R_d}{1 + R_d}Q_b$$

'1 he total dosage of energetic, sputtering ions at the target is [hen

$$N_E = \frac{1}{e}\left(Q_b^{+} + \frac{1}{2}Q_b^{++}\right) \qquad (4)$$

The yield is then given by the ratio of atoms removed to incident energetic ions;

$$Y = \frac{N_A}{N_E} \qquad (5)$$

which can be expressed in terms of the. previous expressions as

$$Y = \frac{h_{eff}}{\left(\int_0^\tau J_p(t)dt - J_{cex}\tau\right)}\left[\frac{\rho e N_{avo}(1 + \gamma_2)(1 + R_d)}{M(1 + \frac{R_d}{2})}\right] \qquad (6)$$

where a constant charge exchange current has been assumed. Although [he. yield given by Eq. 6 is corrected for double ion dosage in terms of the *number* of incident ions, it dots not correct for *damage* caused by the double ions which impact with twice the energy. This is a much more dill icult correction 10 make since one would have 10 have some knowledge of the yield as a function of energy which is what is being calculated. As seen in '1'able. 1, for the operating conditions used in these tests, the fraction of double ions was insignificant,

Inthese experiments the probe (and target) was loc ated only 6.6 cm (2.6 in) from the source.. With the target and source. in such proximity, a potentially significant uncertainty in the measured current is introduced by non uniformit y of the beam profile. During the experiment, the probe is centered on the point of maximum current in the beam. This was checked at various times during the experiment by moving the probe slightly and observing the probe c urrent. The eroded portions of the samples arc located within a 1.27 cm (0.5 inch) diameter circle centered on the probe. Non uniformity of the beam results in the current density decreasing away from the probe. This situation was worsened by localized erosion of the ion source. accelerator grid resulting in the complete erosion of the webbing joining a group of 4 or 5 holes (out of a total of 4-/5 holes) in the grid. The resulting perturbation in the beam symmetry was noticeable in a subsequent mapping of the current profile. 1'0 cone.cl the dose calculation for beam non uniformity, the density profile maps were used to estimate the incident current at the exposed sample as a fraction of the probe or maximum beam, current.

IV, Results

The yield measured for molybdenum is presented in Fig. 3 along with data from Rosenberg and Wehner [5] and Weijsenfeld et al. [6]. Both of the.sc previous studies used plasma sources to provide the incident ions and utilized measurement of target mass loss to determine the quantity of sputtered material. Although a quantitative comparison is difficult without uncertainty estimates for the earlier work, the yields calculated here arc set.n 10 be greater by a factor of 1.3 at 750 eV up to a factor of 3.1 at 150 cV.

The most significant di f ference between the present work and the..sc ealier experiments is that in the present work the, targets were bombarded al non-normal incidence. In a study of the effect of incidence angle on sputter yields, Wehner (Ref. 9) determined that metals generally fall into one of three classes; those exhibiting a 1) "very slight angle effect", 2) "moderate angle effect", and 3) "very pronounced effect". The third group include.s iron, tantalum, and molybdenum. Wehner's data includes sputter yields for molybdenum as a function of incidence angle subject [0 heavy ion sputtering (Hg^+) at energies of 200cV and 800eV. 'I'his data was used to determ inc an empirical relation for the ratio of the yield at some angle relative to that for normal incidence as function of angle and energy;

$$\frac{Y(\theta)}{Y(0)} = f(\theta, E) \quad 0^\circ < \theta < 30^\circ$$

The data corrected using thing this empirical relation is shown in Fig. 3. The sensitivity to incidence angle suggests Ibis is a likely source of the difference in the prc.sent results with those of the previous work. Other possible differences include secondary electron emission, charge exchange, or double ion current collection.

At low energies (<1 kcV) the secondary electron emission is roughly constant and less than 2 percent of the beam current for xenon incident on the tungsten probe [3]. This represents only a small uncertainty. The technique used by Wehner in this previous work, name.ly biasing a target substrate in a plasma would not induce a large charge exchange current since the acceleration of the ions occurs over a relatively small volume (sheath). As a result it is unlikely that he was collecting a significant charge exchange current which he did not correct for. Finally, with respect to damage due to double ions, from the. last two columns in "1'able 1, it is evident that in the present experiment the role of double ions was negligible. This eliminates the possibilty that double ions with twice the kinetic energy could account for the higher yield.

The absolute yield data for all three materials arc presented in Fig. 4, The carbon-carbon yield increases monotonically with energy, as expected from previous investigations with graphite. [5]. Unlike graphite, the carbon-carbon composite consists of graphitic fibers woven together in a carbonaceous matrix, which is in part graphitic and part glassy carbon [7]. Although these targets were polished before testing, examination of the profilometer traces reveal an increase in surface roughness after exposure to the beam, probably resulting from local variation in yield due to non-homogenaities in the material.

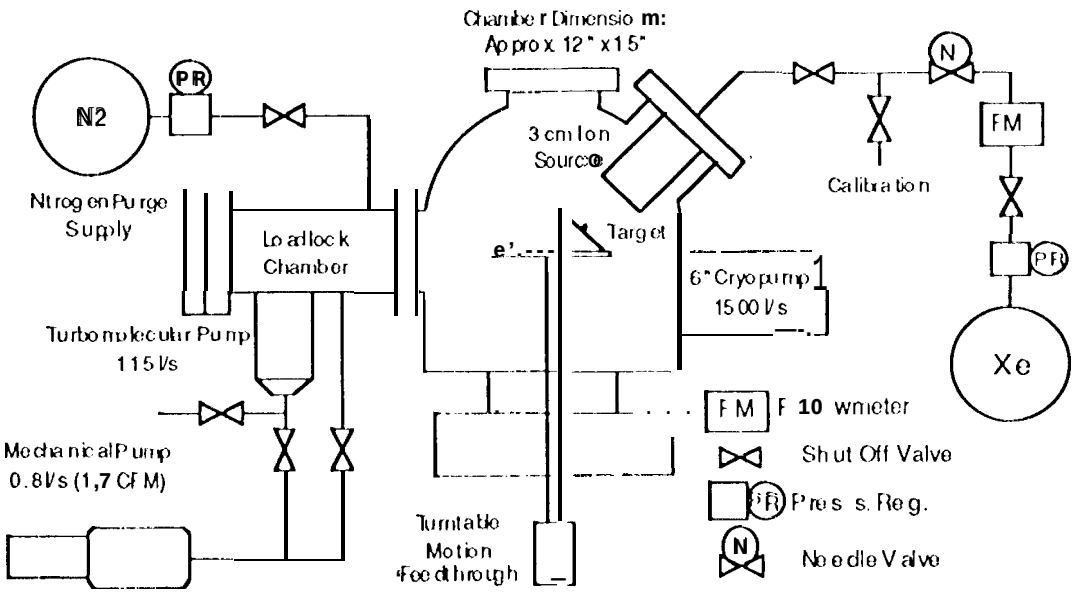

Fig. 2. Schematic of the UI IV test system

Table 1. Base and test pressures, calculated discharge gas utilization efficiency and double to single ion current ratio.

Energy (eV)	Base Press. (Torr x 10(-))	Test Press. (Torr x 10^4)	Gas Utilization Efficiency	J^{++} / J^{+}
150	7.7	2.1	0.022	().00097
250	1.1	2.1	0.06-/	0.00264
500	11.0	2.1	0.088	0.00326
750	2.3	2.1	().()91	0.00340

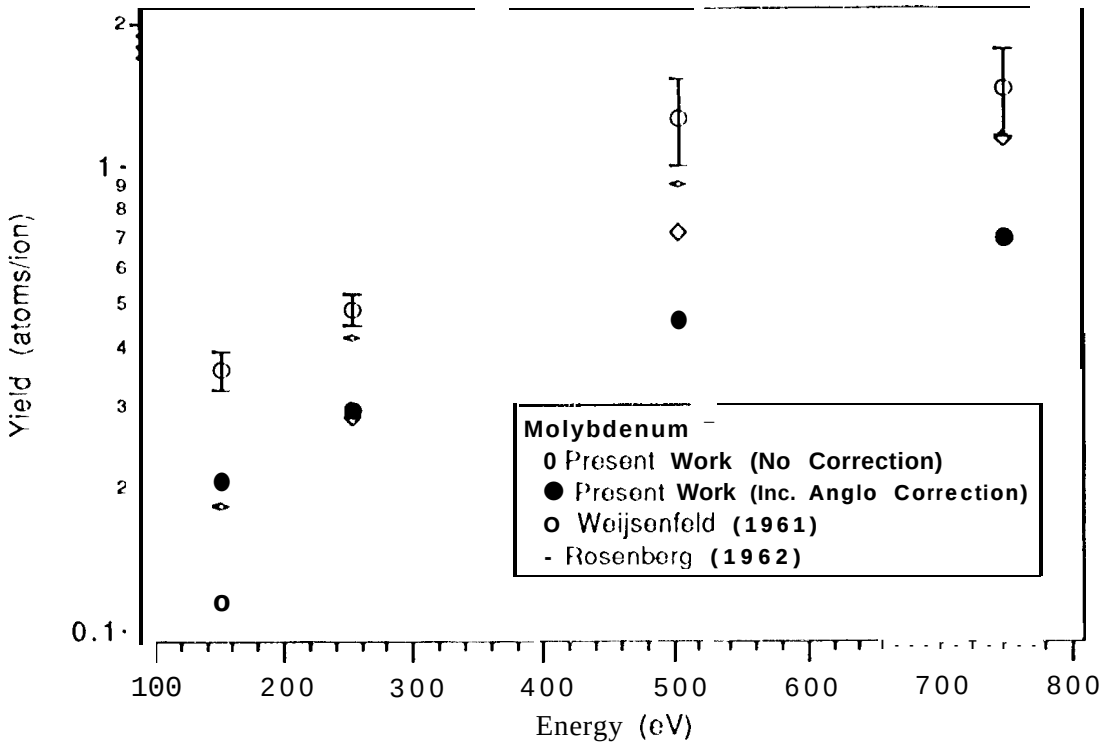

Fig. 3. Comparison of molybdenum yield with data of Weijsenfeld and Rosenberg illustrating pronounced effect of incidence angle. Incidence angles for present work are listed in Table 2.

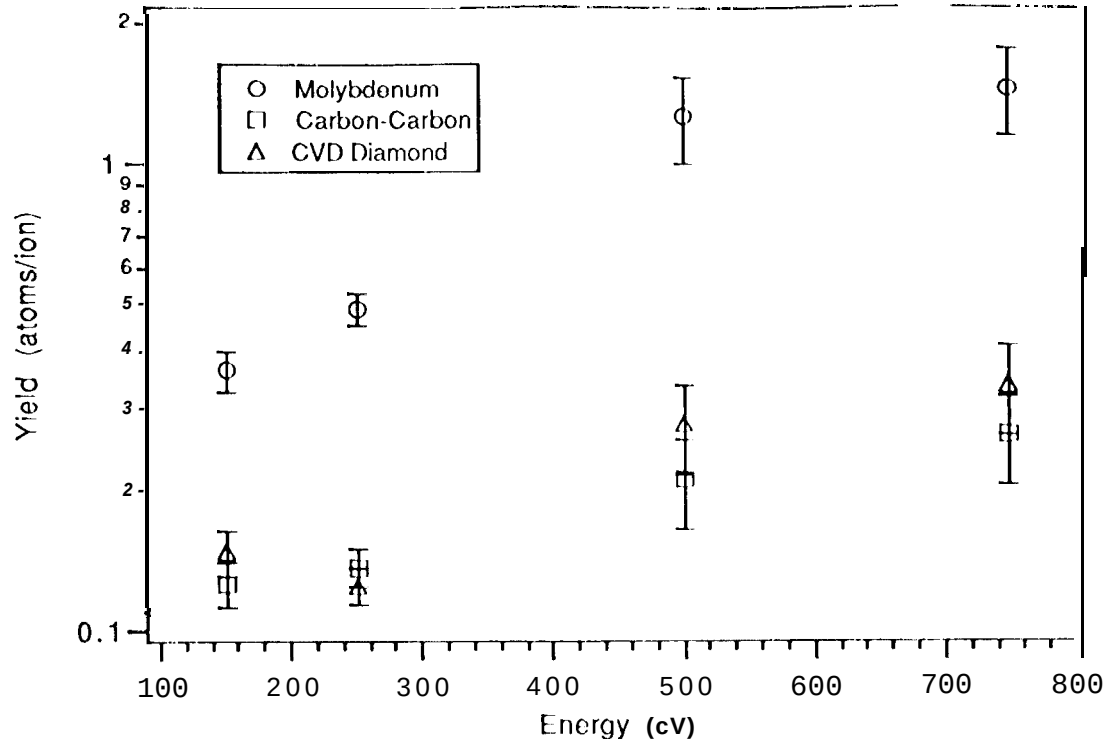

Fig. 4. Sputter Yields for Molybdenum, Carbon-Carbon composite, and CVD Diamond

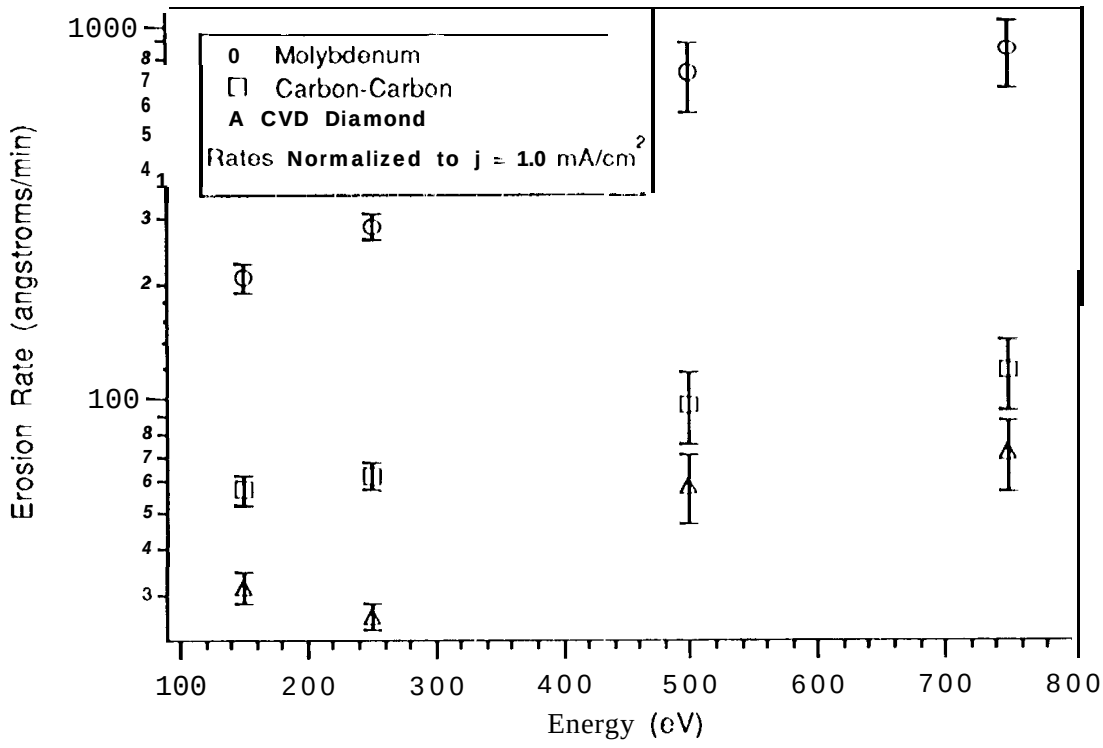

Fig. 5. Erosion Rates for Molybdenum, Carbon-Carbon composite, and CVD Diamond

The yield data for the polycrystalline diamond is lower than expected at an energy of ? 50 eV where it deviates from a monotonically increasing function. Incidence angle data for polycrystalline materials in the keV range suggest a $\cos^{-1}$ dependence [8] in which the yield increases with incidence angle. Referring to Table 2, an incidence angle for this case of 17 degrees would result in a yield close to 10 percent higher than that at normal incidence and therefore does not account for the lower yield. The lower than expected yield is likely due to effects of the surface topography of the sample. To investigate this possibility, the sample was imaged with an SEM in the eroded valleys tori'csponding 10 each of the tests. These photographs reveal a larger density of pits in the surface used for the 150 and 250 CV tests, This face of the sample corresponds 10 the first layer grown in the deposition process which may explain the higher density of pits. It is possible these arc areas where the crystallites had not completely covered the substrate during the growth process. In particular, the valley corresponding to the test at 250 CV is seen to be noticeably rougher with a higher surface density of pits. In gene.ral the yields for rougher surfaces tend to belower due in part to rc-deposition of sputtered material along side.s of surface features.

'1'able 2. Mean current densitiy at target and incidence angle (from normal) averaged over test duration.

Energy (eV)	J (mA/cm^2)	Incidence Angle (deg)
150	0.27 +/- 0.02	14.5
250	0.71 +/- 0.05.	12.2
5(X)	1.63 +/- 0.34	17.4
750	2.56 +/- 0.54	10.2

For engineering calculations the erosion rate is often a more meanigful way to present comparisons of sputtering data since one does not have to correct for differing material densities to assess relative performance. The erosion rate is related to the sputter yield by the following relation;

$$\dot{R} = \frac{h_{eff}}{\tau} = \left(\frac{M}{e \rho N_{AVO}} \right) Y \bar{j} \qquad (7)$$

where $\bar{j}$ is the mean current density average.d over the duration of the exposure. This can be determined from the previous expression for the dosage of energetic ions by

$$\bar{j} = \frac{1}{\tau} \left(Q_b^+ + \frac{1}{2} Q_b^{++} \right) = \frac{e}{\tau} N_E \qquad (8)$$

The erosion rate results for the three materials arc presented in Fig. 5 with value.s normalized to a current density of 1 mA/cm^2.

V. Conclusions

Sputter yields were measured for molybdenum, carbon-carbon, and polycrystalline diamond subject to xenon ion bombardment in the energy range of 150 to 750 eV. Erosion rates were calculated for each case corresponding to a normalized current density of 1 mA/cm^2. The ratio of erosion rate for diamond relative to molybdenum and carbon-carbon is listed in Table 3. The ratio at 250 eV is high duc to the lower than expected erosion rate of the polycrystalline sample as previously discussed. The conclusion from these. measurements is that CVD diamond can decrease the erosion rate by roughly 40 percent relative to carbon-carbon, and 85 - 92 percent relative 10 molybdenum.

Table 3. Ratio of Erosion rates for molybdenum and carbon-carbon relative to diamond.

Energy (eV)	$\frac{\dot{R}_{Mo}}{\dot{R}_{Dia}}$	$\frac{\dot{R}_{C-C}}{\dot{R}_{Dia}}$
150	6.8 +/- 3.5	1.8 +/-1.3
250	10.8 +/- 3.5	2.4 +/- 1.3
500	12.5 +/- 3.5	1.6 +/- 1.3
750	11.8 +/- 3.5	1.7 +/- 1.3

As was discussed in Ref. 2, two appraches arc under consideration to utilize the lower erosion rates for diamond. One is to coal a molybdenum (or possibly carbon-carbon) grid with a diamond film, the second is to fabricate the grid from a relatively thick (1 mm) free standing film. The extent to which grid life.tirnc can be increased will strongly depend on which of these two approaches is adopted because a coating tens of microns thick will eventually be eroded through. However, given the number of companies which currently perform high quality diamond film coatings (especially on molybdenum substrates), the benefits in increased lifetime suggested by the data arc wor h persuing.

VI. Acknowledgments

The work described in this paper was performed by the Jet Propulsion Laboratory (JPL), California Institute of Technology, under contract with the National Aeronautics and Space Administration.

The authors wish to express their thanks to the many individuals who helped make this work possible. In particular, Dr. Marc Nicolet for making the Sputter Deposition Laboratory available to us, Dr. Richard Koba of Crystalline Materials Corp. for providing the synthetic

diamond sample used in this work, and Dr. John Brophy for his invaluable assistance with the analysis and interpretat ion of the data.

VII, References

1. Spear, K.E., "Dian]ond-Ceramic Coating of the Future", J. Am. Ceram. Sot. 72(2), 1989, pp. 171-191.

2. Blandino, J. J.,Goodwin, D.G., Garner, C. R., Brophy, J.R.,"Evaluat ion and Development of Diamond Grids for Ion optics", AIAA 95-2663, Presented at the 31st Joint Propulsion Conference, July 10-121995 San Diego, CA.

3. Hagstrum, H.D., "Effect of Monolayer Adsorption on the. Ejection of Electrons from Metals by Ions", Physical Review, 104(6), 1956, pp. 1516-1527.

4. Efremow, N. N., Geis, M. W., Flanders, D.C., Lincoln, G. A., and Economou N. P., "Ion Beam Assisted Etching of Diamond", J. of Vat. Sci. Technol. B 3(1), Jan/Feb 1985, pp. 416-418.

s. Rosenberg, D. and Wehner, G.K., "Sputtering Yields for 1.OW Energy He, Kr, and Xc Ion Bombardment", J. App. Phys. 33(5), 1962, pp. 1842- 1845.

6. Weijsenfeld, C.}]., Hoogendoorn, A., and Koedam, M. "Sputtering of Polycrystalline Metals by Inert Gas ions of Low Energy (100 - 1000 eV)", Physics, 27, 1961, pp. 763-764.

7. Mueller, J., Brophy, JR., and Brown D.K., "Endurance Testing and Fabrication of Advanced 1 S-cm and 30-cm Carbon-Carbon Composite Grids", AIAA 95-2.660, Presented at the 31st Joint Propulsion Con ference, July 10-121995 San Diego, CA.

8. Behrisch, R. , Ed. Sputtering by Particle Bombardment I; Physical Sputtering of Single-Element Solids, Springer-Verlag Berlin Heidelberg, 1981, pp. 200-203, 219-222.

9. Wehner, G. "Influence of the Angle of Incidence on Sputtering Yields", J. App. Phys. 30(1 1), 1959, pp. 1762- 1765.

10. Brophy, J. "ion Thruter Performance Model", NASA-(X-174810, Dec. 1984.